

Revealing the Size-dependent Electrochemical Li-storage Behaviors of SiO-based Anode

Yang Li,^a Hongmin Zhou,^b Ning Lin ^{*a} and Yitai Qian ^a

[a] Department of Applied Chemistry, University of Science and Technology of China, Hefei 230026, China

[b] Instruments Center for Physical Science, University of Science and Technology of China, Hefei 230026, China

E-mail: ningl@mail.ustc.edu.cn

Experimental

Materials synthesis

Airflow mill and classification-screening system was used to obtain micro-sized and submicro-sized SiO powders. The as-prepared SiO powders were dispersed on a quartz plate and placed inside the chemical vapor deposition (CVD) furnace. The SiO powders were maintained at 900 °C under a mixed gas flow of argon and methane for carbon coating. After the furnace was cooled to room temperature, black micro-sized and submicro-sized SiO@C powders were obtained.

Electrode and cell fabrication

SiO-based electrode was composed of 80 wt.% active materials, 10 wt.% super P, 10 wt.% carboxymethyl cellulose. The graphite/SiO@C blend electrodes were composed of 90 wt.% active materials (graphite : SiO@C = 95 : 5; 90 : 10; 80 : 20; 70 : 30 and 50 : 50 in mass ratio), 5 wt.% super P, 5 wt.% carboxymethyl cellulose. The slurry was coated on copper film and dried at 100 °C for 6 h in a vacuum oven. The electrodes were punched into 12 mm disks for use. The mass loading of the active materials on each SiO electrode and graphite/SiO blend electrode were $0.8 \pm 0.1 \text{ mg cm}^{-2}$ and $3.0 \pm 0.1 \text{ mg cm}^{-2}$, respectively. The electrochemical properties were measured using coin-type 2016 cells, which were assembled in the argon-filled glove box. For the Li | SiO@C and Li | graphite/SiO@C cells, lithium foil acted as the counter electrode, a solution of 1 M LiPF₆ in a mixture of ethylene carbonate/diethyl carbonate (EC/DEC; 1:1 by volume) with 10 wt.% fluoroethylene carbonate (FEC) and 2 wt.% vinylene carbonate (VC) was used as the electrolyte and Celgard 2400 membrane was applied for a separator. The galvanostatic charge/discharge properties were tested on LANDCT2001A at different current densities in a voltage window of 0.005-2.0 V. The electrochemical impedance spectroscopy (EIS) were performed on a CHI 660D electrochemical workstation.

Structural and electrochemical characterizations

The X-ray diffraction (XRD) patterns of the samples were obtained from Philips X'Pert Super diffractometer with Cu K α ($\lambda=1.54182$ Å). Raman spectra were characterized using JYLABRAM-HR Confocal Laser Micro-Raman spectrometer at 532 nm. The morphologies of the samples were performed on scanning electron microscopy (SEM, GeminiSEM 500), transmission electron microscopy (TEM, Hitachi H7650) and high resolution transmission electron microscopy (HRTEM, JEM-2100F). The surface areas and pore size distribution of the samples were characterized using BEL SORP-max machine (BEL, Japan). Thermogravimetric analysis (TGA) curves were obtained from Shimadzu TGA-50H. X-ray photoelectron spectra (XPS) were collected on an ESCALAB 250 X-ray photoelectron spectrometer (Perkin-Elmer). Time-of-flight secondary ion mass spectrometry (TOF-SIMS) analysis was carried out with a TOF-SIMS 5 spectrometer (ION-TOF GmbH). A 1000 eV Cs⁺ (negative) ion beam was used to sputter the cycled electrodes (Area: 300 * 300 μm^2). In SEM, XPS and TOF-SIMS tests, air-sensitive electrodes were transferred to test chambers in a special argon gas shield to ensure the reliability of the data.

The calculation of expansion rate

Let the space area before expansion be V , the area after expansion is V' , take $o \in V$ as the origin, and choose three orthogonal directions to establish a Cartesian coordinate system. The volume before expansion is:

$$|V| = \iiint_{(x,y,z) \in V} 1 dx dy dz$$

$\forall a = (x,y,z) \in V$, Let the corresponding point after expansion be a' . From the definition of uniform expansion, $a' - o' = \alpha(a - o)$, where α is the expansion rate.

$$\therefore a' = (x', y', z') = (\alpha x, \alpha y, \alpha z)$$

$$J = \frac{\partial(x', y', z')}{\partial(x, y, z)} = \begin{pmatrix} \alpha & 0 & 0 \\ 0 & \alpha & 0 \\ 0 & 0 & \alpha \end{pmatrix}$$

$$dx' dy' dz' = |J| dx dy dz = \alpha^3 dx dy dz$$

Then the expanded volume is:

$$|V'| = \iiint_{(x', y', z') \in V'} 1 dx' dy' dz'$$

$$= \iiint_{(x, y, z) \in V} \alpha^3 dx dy dz$$

$$= \alpha^3 \iiint_{(x, y, z) \in V} 1 dx dy dz \\ = \alpha^3 |V|$$

$$\alpha = \frac{\alpha_1 + \alpha_2 + \alpha_3 + \alpha_4 + \alpha_5 + \alpha_6}{6} = \frac{1.338 + 1.381 + 1.333 + 1.348 + 1.360 + 1.340}{6} = 1.350$$

$$\alpha^3 = 2.460$$

The materials characterizations

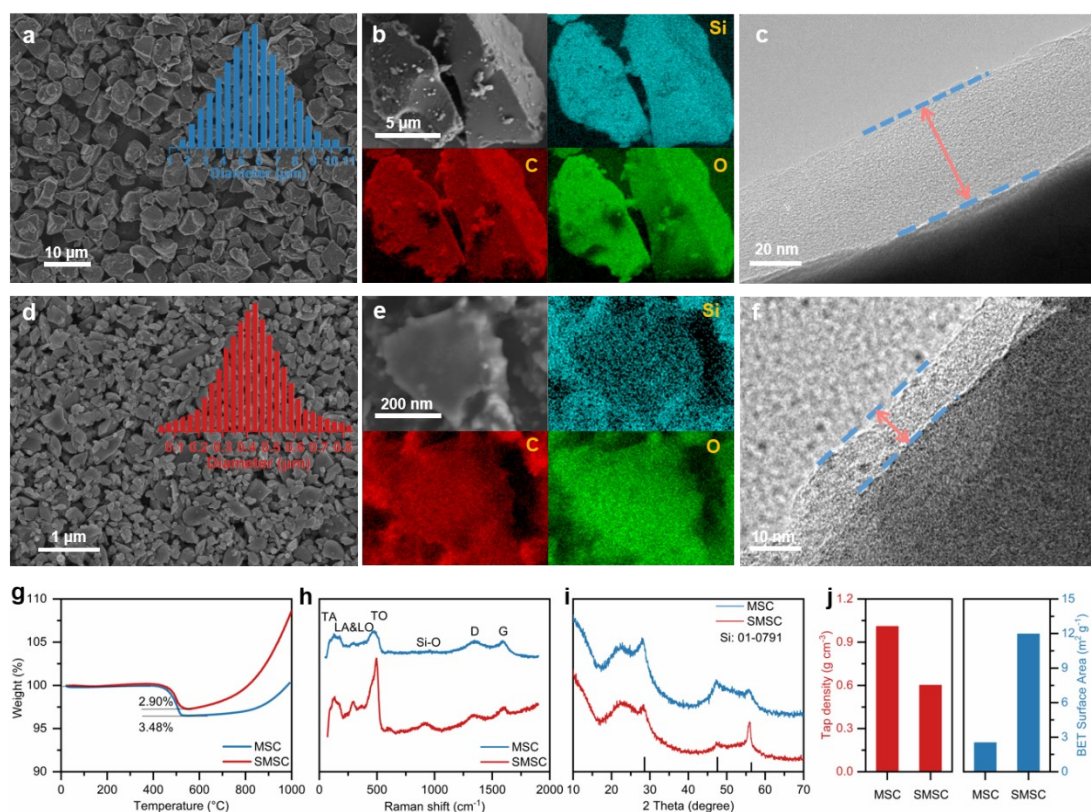


Figure S1. The SEM image, particle size distribution (a), EDS mapping (b) and TEM image (c) of micro-sized SiO₂ powders.; The SEM image, particle size distribution (d), EDS mapping (e) and TEM image (f) of submicro-sized SiO₂ powders.; The TGA curves (g), Raman spectra (h), XRD pattern (i), tap density and BET surface area (j) of micro-sized and submicro-sized SiO₂ powders.

Figure S1a-f show the SEM, the corresponding EDS mapping and TEM pictures of the obtained powders. As one can see, the particle size of MSC is uniform and centered at about 5.75 μm , and the particle size of SMSC is ranging from 255 nm to 555 nm. The EDS mapping pictures exhibit that a dense and uniform carbon layer is deposited on the surface. The thickness of the carbon layer in MSC is about 30 nm, and that in SMSC is about 8.5 nm. The weight ratio of carbon layer is determined by thermogravimetric analysis plots to be 3.48% (MSC) and 2.90% (SMSC) (**Figure S1g**). The Raman spectra confirm that the carbon layer is amorphous and the SMSC has more obvious characteristic peaks of SiO₂ due to more interface exposure compared with MSC (**Figure S1h**). Both samples present similar XRD patterns, the Si domains within the SiO₂ particle is about 2.1 nm on basis of the Scherrer equation (**Figure S1i**). On basis of the nitrogen adsorption/desorption isotherms (**Figure S2**), the calculated

Brunner–Emmet–Teller surface area of the MSC and SMSC are calculated to be 2.51 and 11.95 m² g⁻¹. In addition, the tap density of MSC sample is 1.01 g⁻¹ cm³ and the tap density of SMSC sample is 0.60 g⁻¹ cm³ (**Figure S1j**).

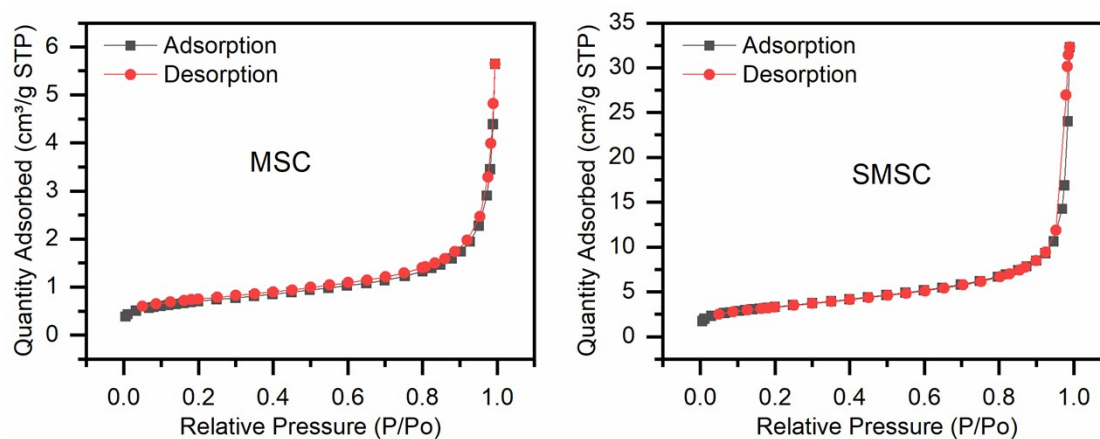


Figure S2. The nitrogen adsorption/desorption isotherms of MSC and SMSC.

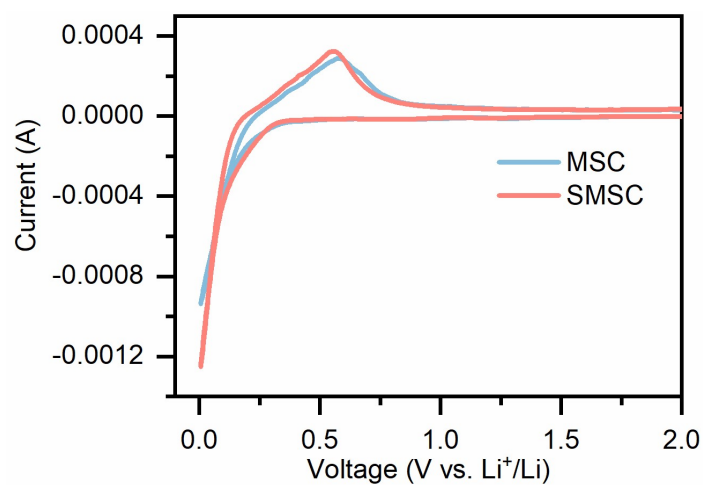


Figure S3. The CV curves of MSC and SMSC for first cycle.

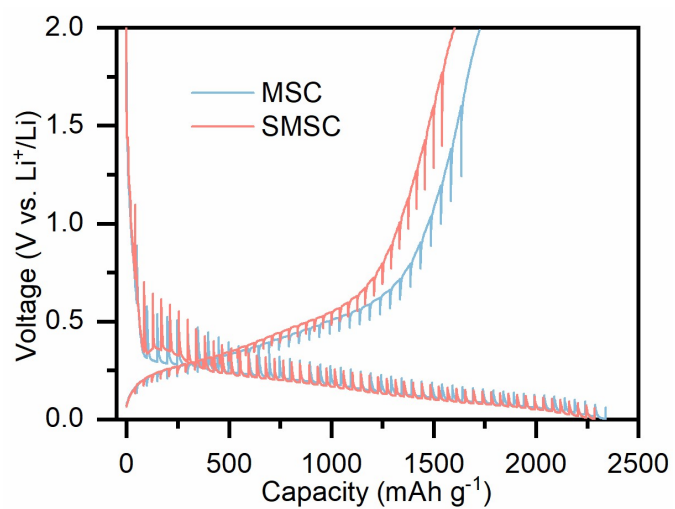


Figure S4. The GITT curves of MSC and SMSC for first cycle.

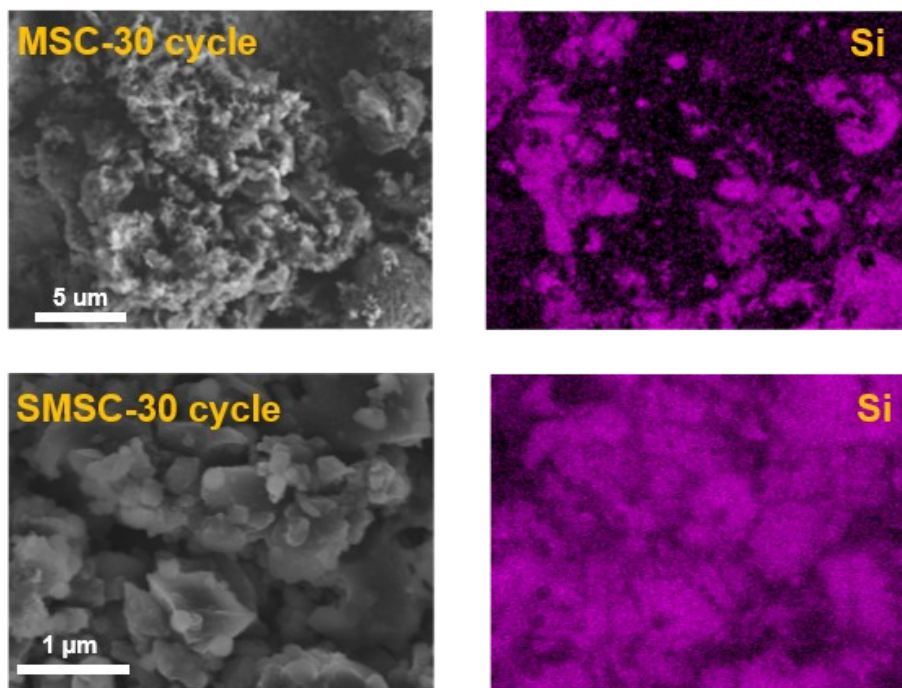


Figure S5. The SEM images and corresponding mapping images of MSC and SMSC after 30 cycles.

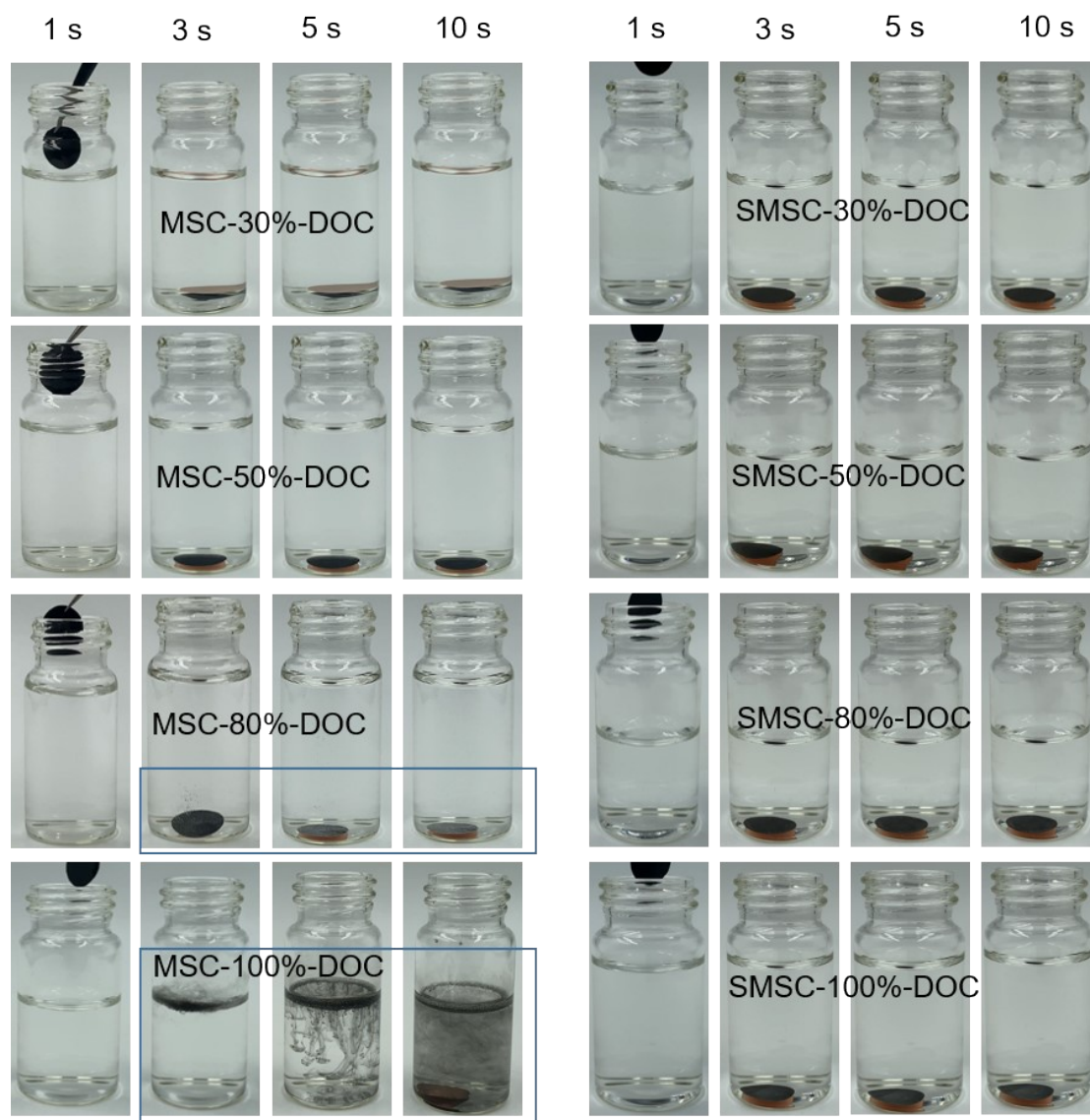


Figure S6. The phenomenon of putting the fully-delithiated electrodes into distilled water.

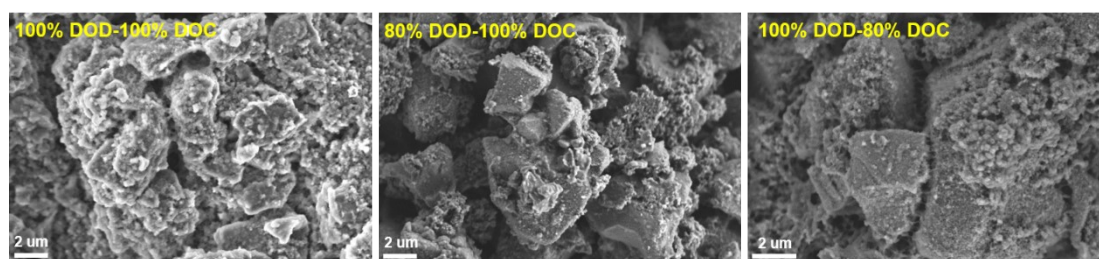


Figure S7. The comparison of SEM images of micro-SiO particles interface and integrity at different charge-discharge depths.

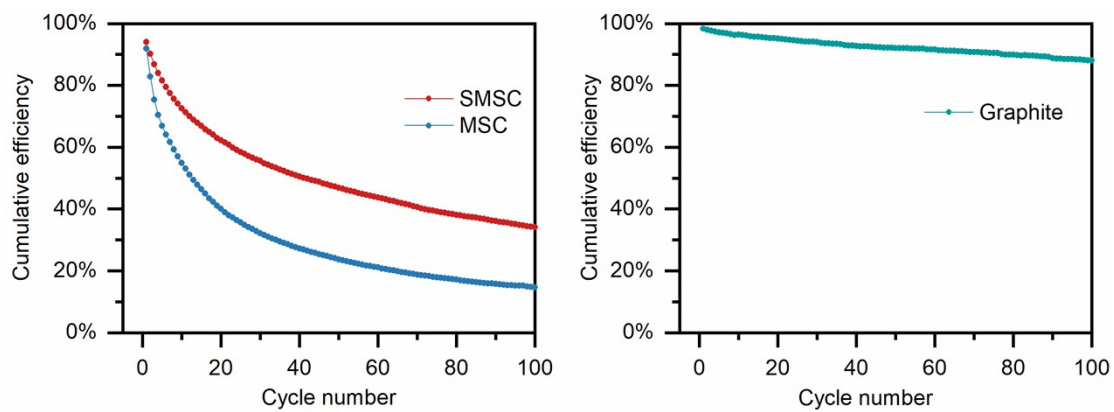


Figure S8. The Comparison of cumulative efficiency of SMSC, MSC and graphite.

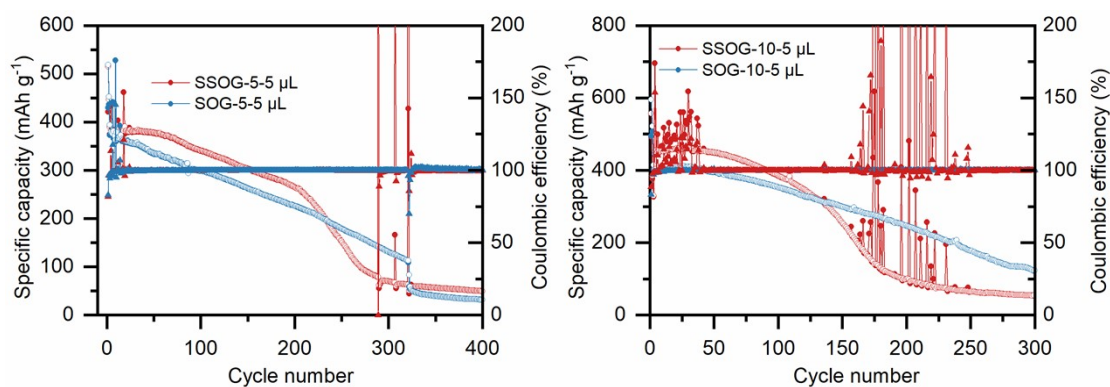


Figure S9. The Comparison of cycle performance of SOG-5/10 and SSOG-5/10 electrodes under limited electrolyte usage.